Smart Tungsten-based Alloys for a First Wall of DEMO

Andrey Litnovsky[a*], Janina Schmitz[a,b], Felix Klein[a], Karen De Lannoye[a,c], Sophie Weckauf[a], Arkadi Kreter[a], Marcin Rasinski[a], Jan W. Coenen[a], Christian Linsmeier[a], Jesus Gonzalez-Julian[a], Martin Bram[a], Ivan Povstugar[d], Thomas Morgan[e], Duc Nguyen-Manh[f], Mark Gilbert[f], Damian Sobieraj[g] and Jan S. Wróbel[g]

[a]Forschungszentrum Jülich GmbH, Institut für Energie und Klimaforschung, 52425 Jülich, Germany
[b]Department of Applied Physics, Ghent University, 9000 Ghent, Belgium
[c]Vrije Universiteit Brussel, 1050 Elsene, Belgium
[d]Forschungszentrum Jülich GmbH, Zentralinstitut für Engineering, Elektronik und Analytik (ZEA 3 Analytik, 52425 Jülich, Germany
[e]DIFFER Dutch Institute For Fundamental Energy Research, De Zaale 20, 5612 AJ Eindhoven, The Netherlands
[f]CCFE,United Kingdom Atomic Energy Authority, Culham Science Centre, Abingdon, Oxfordshire OX14 3DB, United Kingdom
[g]Faculty of Materials Science and Engineering, Warsaw University of Technology, Wołoska 141, 02-507 Warsaw, Poland

During an accident with loss-of-coolant and air ingress in DEMO, the temperature of tungsten first wall cladding may exceed 1000°C and remain for months leading to tungsten oxidation. The radioactive tungsten oxide can be mobilized to the environment at rates of 10 - 150 kg per hour. Smart tungsten-based alloys are under development to address this issue. Alloys are aimed to function as pure tungsten during regular plasma operation of DEMO. During an accident, alloying elements will create a protective layer, suppressing release of W oxide.

Bulk smart alloys were developed by using mechanical alloying and field-assisted sintering technology. The mechanical alloying process was optimized leading to an increased powder production by at least 40%. Smart alloys and tungsten were tested under a variety of DEMO-relevant plasma conditions. Both materials demonstrated similar sputtering resistance to deuterium plasma. Under accident conditions, alloys feature a 40-fold reduction of W release compared to that of pure tungsten.

Keywords: DEMO, passive safety, tungsten alloys, suppressed oxidation, plasma-facing material, yttrium.

1. Introduction and motivation

In a future fusion power plant, such as the DEMOnstration Power Plant (DEMO) safety of operation will be of highest importance [1,2]. Presently, due to a number of advantages, such as a high melting point, low sputtering by plasma particles, relatively short-term activation, low tritium retention and high thermal conductivity, tungsten (W) is deemed as a preferred candidate material for a plasma-facing first wall. At the same time, assessment of accident conditions revealed severe issues with using pure tungsten [3]. In the case of a loss-of-coolant accident, accompanied by air ingress into the vacuum vessel, tungsten first wall would be in contact with surrounding atmosphere. In the absence of a coolant, the temperature of the tungsten cladding can climb to 1000°C and even higher due to the nuclear decay heat and remain at such a level for weeks [3]. At such temperatures, neutron-activated tungsten and its radioactive isotopes, will form volatile oxides. According to calculations made for DEMO [4], the amount of radioactive oxides sublimated into atmosphere from the first wall will be in the range of 50-150 kg/hour. Such a dramatic radioactive release must be suppressed to the highest possible extent.

Self-passivating tungsten based alloys were originally proposed and developed by Koch and Bolt [5–7]. These, so-called "Smart Alloys" (SA), change their properties depending on environment. During regular plasma operation, the lighter alloying elements such as chromium (Cr), zirconium (Zr) or yttrium (Y) will be more easily sputtered by plasma particles leaving almost a pure W surface facing the plasma and having all the aforementioned advantages of pure tungsten. During an accident, the remaining alloying elements in the bulk will diffuse to the surface and form their own oxides protecting tungsten from oxidation and subsequent sublimation into atmosphere.

Recent studies have shown the benefits of W-Cr-Y systems [4,8,9]. These SA have demonstrated greatly superior oxidation resistance. The research formerly based on laboratory-scale thin films, has been rapidly changed towards bulk samples. Usually, mechanical alloying (MA) [10] was used to obtain the SA. The samples were produced by using hot isostatic pressing [11]. Recently, field-assisted sintering technology (FAST) [12] was applied for the production of bulk samples, reducing the time necessary for the compacting and sintering of alloyed powders down to minutes [9,13]. New SA systems produced using FAST featured superior oxidation properties [9,13–15] and acceptable plasma performance [16–19]. The technology of production was treated as advanced enough to allow material performance tests on the timescale of their expected lifetime in DEMO.

E-mail: a.litnovsky@fz-juelich.de

In this paper, further optimization of the mechanical alloying route is explained followed by the results of the plasma tests of the SA under DEMO-relevant conditions. These investigations are accompanied by the assessment of bulk SA under accident conditions in DEMO. A summary of results and an outlook to future studies conclude the paper.

2. Optimized mechanical alloying

Mechanical alloying is a standard technique used for the production of bulk systems. The elemental powders, in our case, W, Cr and Y, are placed in a milling jar with tungsten carbide balls and then milled for several hours using a planetary mill. In the case of successful milling, the resulting powder represents the W-Cr alloy without residual W and Cr constituents. With the commissioning of a new powder metallurgical lab, the PowderLab at Forschungszentrum Juelich GmbH, the new planetary mill Retsch PM 400 became available. In contrast to previously used PM 400 in former studies, the new mill features higher rotational ratio 1: (-3). In this ratio, the first number is the normalized speed of base in a planetary system. The second number is a normalized speed of the milling jar with respect to the base. Higher rotational ratio allows the transfer or more energy to the powder i.e. it may potentially result in better and faster alloying. On the other hand, higher power exerted to the powder may lead to pressing the powder to the jar´s walls and as a consequence, to incomplete milling. Other important parameters for milling are the ball-to-powder ratio (BPR) and the free remaining volume. The former mainly influences the intensity of the mechanical contact between the powder and the balls i.e. the efficiency of energy transfer to the powder. The latter parameter is important for ensuring that a sufficient amount of energy is transferred during a single contact of the powder with a milling ball.

Based on the aforementioned expectations, a parametric optimization was made. During such an optimization, usually one milling parameter was varied while all the remaining ones were fixed. The tungsten carbide milling jars with a total volume of 250 ml. were used for optimization. The rotation speed of the milling base was kept at 250 rpm. Unless otherwise stated, the reported results were obtained via milling for 60 hours using the 10 mm balls of tungsten carbide. The quality of the alloying was investigated using the Bruker Discover D8, X-Ray diffraction system at FZJ. The current results of the optimization are shown in Table 1.

As can be seen from the table, experiments 1 and 2, copying of the milling parameters from the former planetary mill did not result in complete mechanical alloying. Interestingly enough allowing smaller milling balls into the jar did not bring any advantages in milling, experiment 7. The most promising results were obtained by either reducing the free volume necessary for alloying (experiment 3) or by reducing the BPR i.e. by allowing more powder in the milling jar (experiment 5). With new parameters of mechanical alloying, it was possible to attain at least 40% more of the fully alloyed powder per one milling session, experiments 3 and 5. In the next optimization step the milling time was reduced from 60 to 30 hours, assuming the quality of alloying will not degrade. The corresponding optimization is ongoing, the first results are available (experiment 9) and investigations on samples created with a new milling scenario is underway.

3. Plasma performance under DEMO-relevant conditions: lifetime tests

Previous studies have already demonstrated good sputtering resistance of developed smart alloys at ion energies below sputtering threshold of W [17,19]. As expected, the alloying elements on the plasma-facing surface were sputtered, whereas the pure tungsten layer remained. Such a tungsten layer provided a protecting action for the underlying smart alloy so that the resulting sputtering resistance of SA and pure tungsten becomes very similar. These experiments, previously performed in linear plasma device PSI-2 [20], were recently continued in the Magnum-PSI linear plasma facility [21], hosted by the Dutch Institute of the Fundamental Energy Research (DIFFER) in Eindhoven, The Netherlands.

Table 1. Results of MA optimization

No.	BPR	Free volume, ml	Powder amount after milling, g	Result
1.	5:1	195	110	old mill, reference regime, complete alloying
2.	5:1	195	110	new mill, repetition of a reference regime, incomplete alloying
A. Reducing the free volume				
3.	5:1	172	156	complete alloying
B. Changing BPR				
4.	3:1	195	168	incomplete alloying
5.	2:1	195	232	complete alloying risk of non-alloyed powder pressed to the jar
C. Attempting to find an optimum combination				
6.	2:1	160	385	Non-alloyed powder pressed on the jar
7.	3:1	195	169	Incomplete alloying, 10 and 5 mm milling balls
8.	3:1	192	179	Complete alloying, milling time 70 hours
Shorter milling with reduced free volume from A.				
9.	5:1	172	156	Complete alloying, milling time 30 hours.

The basic arrangements of plasma exposures applied during earlier experiments on PSI-2 [17,19] remained.

The SA and pure W samples were exposed to the steady-state deuterium plasma under as similar as possible conditions. Plasma parameters were monitored using the moveable Langmuir probe in PSI-2, whereas in Magnum-PSI the Thomson scattering was employed for such a purpose [22]. The temperature of the samples was surveyed in PSI-2 using the multi-zone infrared camera (FLIR) calibrated using the thermocouple mounted beneath one of the samples. In experiments on Magnum-PSI the temperature of samples was monitored using a spectroscopic pyrometer.

In all experiments, the sample temperature was kept in the range 620°C-700°C i.e. at the temperature expected for the first wall in DEMO. In all experiments, the ion energy was about 120 eV, which was attained by active biasing of the samples. During all exposures, the SA and tungsten samples were placed at the position of the maxima of corresponding electron density and temperature. A key difference in the exposures on both machines was the way the samples were exposed. In PSI-2, all SA and W probes were exposed simultaneously (Fig. 1a) under identical plasma conditions [17] taking an advantage of a hollow plasma profile and rather large diameter of a plasma column. In in Magnum-PSI only one sample can be exposed at once, see Fig.1b. Therefore, in order to ensure the direct comparison between pure tungsten and smart alloys, pairs of identical exposures at the same plasma fluence were conducted for SA and W samples for each fluence. Exposures in Magnum-PSI brought advantages of reaching the higher fluxes and hence, attaining higher fluence.

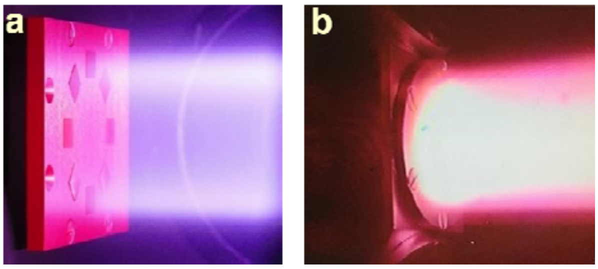

Fig. 1. Photographs of plasma exposures in linear devices: a) simultaneous exposure of smart alloy and pure tungsten samples in linear device PSI-2 and b) consecutive one-by-one exposure in MAGNUM Psi.

Here, we introduce the following nomenclature of experiments, which will be followed in our subsequent papers. The first capital letter designates the main plasma ion species; the following number represents the ion energy in eV, the capital letter afterwards, e.g. "P" or "M" stays for the facility: "P" for PSI-2 and "M" for Magnum-PSI. The last letter is the number of the particular experiment. As an example, "D120P2" would mean the second experiment performed on PSI-2 with deuterium plasma, having ion energies around 120 eV.

The main parameters and the results of exposures are summarized on Table 2. In Magnum-PSI it was possible to obtain the highest plasma fluence of $2.0\text{x}10^{27}$ ion/m^2.This is a factor ~ 12 higher than the highest one attained in PSI-2. Taking into account the estimates for expected fluxes on the first wall in DEMO [23], the highest attained fluence corresponded to that in about 20 days of continuous DEMO operation. The experiments in Magnum-PSI have confirmed a similarity of sputtering resistance of W-Cr-Y smart alloys and pure tungsten.

The ratio of the mass of removed material both from the W and SA samples was estimated taking into account the same surface recession caused by sputtering of both SA and W samples and using the theoretical density of SA of 15.9 g/cm^3 [24]. The theoretical ratio $\Delta m_W/\Delta m_{SA}$ is 0.82. As can be seen from the table 2, the actual ratios measured in the course of all exposures match the theoretical value very well. The only exclusion detected for an experiment D120M1 was due to a very short exposure time and hence, a larger uncertainty of results. Generally, a good agreement between the modeled and experimental ratios of mass loss for SA and pure W evidences an absence of additional loss of alloying elements during the described plasma exposures. Thus, clear evidences of the feasibility of plasma operation with smart alloys as plasma-facing material were obtained.

At the same time, the exposures performed at energies above the sputtering threshold of tungsten and exposures made with seeded plasmas have shown unfortunately, a vulnerability of both W and SA [17,18]. Certainly, these questions need to be addressed in greater details in future. The preparation of the overview of plasma performance of smart alloys is presently underway.

Table 2. Main parameters and results of plasma exposures in PSI-2 and Magnum-PSI linear devices.

<table>
<tr><th>Experiment</th><th>Fluence, ion/m^2</th><th>Sample temperature, °C</th><th>Δm_W/ Δm_{SA}</th><th>Results</th></tr>
<tr><td>D120P1</td><td>$1.0\text{x}10^{26}$</td><td>620-700</td><td>0.81</td><td rowspan="6">Similar sputtering of W and SA. Protecting W layer on the surface of SA. Insignificant change of morphology. Low deuterium retention of order of $1\text{x}10^{14}$ D/cm^2 in PSI-2 [24]</td></tr>
<tr><td>D120P2</td><td>$1.7\text{x}10^{26}$</td><td>620-700</td><td>n.a</td></tr>
<tr><td>D120M1</td><td>$1.0\text{x}10^{26}$</td><td>630-670</td><td>0.62</td></tr>
<tr><td>D120M2</td><td>$5.0\text{x}10^{26}$</td><td>630-670</td><td>0.89</td></tr>
<tr><td>D120M3</td><td>$1.0\text{x}10^{27}$</td><td>630-670</td><td>0.83</td></tr>
<tr><td>D120M4</td><td>$2.0\text{x}10^{27}$</td><td>630-670</td><td>0.82</td></tr>
</table>

4. Smart alloys under accident conditions

Ensuring good performance under the expected severe accident conditions is another fundamental condition in ensuring the viability of smart alloys. For this purpose, several studies were performed on controlled oxidation of smart alloys in the air-containing atmosphere in a dry and later on, in a humid environment [13–15,25–27]. The aim of these studies is to evaluate the oxidation resistance of smart alloys under conditions as close as possible to those expected during opening of a fusion power plant to the atmosphere in the case of a severe accident as described in the introduction. All studies were performed in the thermogravimetric (TGA) facility Setaram TAG 16/18 equipped with the steam generator Setaram WetSys located in the ThermoLab [28] in Forschungszentrum Jülich.

Usually, in the course of controlled oxidation the mass increase of a sample caused by oxidation is recorded. The radioactive hazard in the fusion power plant will not however, be directly caused by oxidation. It is sublimation of oxidized tungsten and transmutation elements, which is responsible for a radioactive hazard. Recently, the TGA facility in Jülich was upgraded in such a way, that direct measurements of sublimation became possible [15], to our knowledge for the first time. The time evolution of the mass decrease due to sublimation from smart alloy is presented in Fig. 2. The smart alloy sample was exposed in an atmosphere containing 20 vol.% of synthetic humid air and 80 vol. % of argon. The sample was kept at 1000°C during the exposure. The synthetic humid air having 70 relative % of humidity was fed at a temperature of 40°C to the SA sample. The resulting mass loss due to sublimation is presented via curve A on figure 2 Curve B represents the tungsten oxide sublimation as measured in fully oxidized tungsten thin film. Curve C shows the sublimation mass loss for the tungsten oxide released from the bulk pure tungsten sample. Curves B and C therefore, create an area where we could expect the WO_3 sublimation from the pure tungsten sample.

As mentioned in [15] with the present setup of the TGA it was impossible to detect any Cr sublimation. Only W sublimation could be detected. The sublimation curve A from the smart alloy therefore, represents only the W sublimation out of the surface of the smart alloy. In order to evaluate the possible maximum contribution of chromium sublimation, a reference model chromium thin film was fully oxidized and then the sublimation of chromium oxide was measured. The conditions of exposure were identical to those described above. The resulting evolution of mass loss due to Cr sublimation is presented via curve D in figure 2. The comparative analysis of the W sublimation from the smart alloys and from the pure W samples yields more than 40-fold suppression of W release on the time scale of 10 days, outlining the remarkable performance of bulk smart alloys produced by FAST under accident conditions.

Recent studies of the surface morphology were undertaken using the Carl Zeiss CrossBeam XB 540 combined scanning electron microscope (SEM) – focused ion beam device equipped among others, with the Energy-Dispersive X-Ray spectroscopy (EDX) system for an elemental analysis. The SEM photograph of the surface of SA after 10 days of exposure in humid air is presented in figure 3. The evaluation of the EDX mapping yielded to less than 1% surface coverage by the mixed W-Y oxides in a remarkable contrast to the full WO_3 surface coverage of the pure tungsten.

The operation scenario for smart alloys in the power plant assumes plasma exposure during regular operation prior to unlikely, but possible exposure in accident conditions. The oxidation studies of plasma-exposed samples are ongoing continuously, the results are published in e.g. [9]. The results of the extensive testing of smart alloys produced using the optimized alloying will be a subject of the dedicated publication.

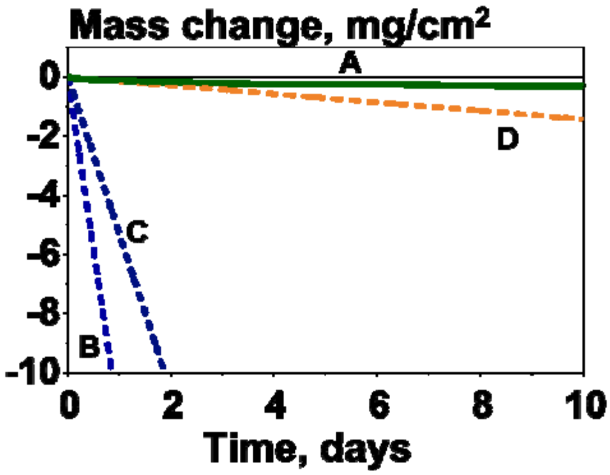

Fig. 2. Mass reduction due to sublimation as a function of exposure time for W-Cr-Y smart alloy (curve A), fully oxidized tungsten thin film (curve B), oxidized bulk W sample (curve C) and for oxidized pure Cr film (curve D) in humid air at 1000°C.

5. Summary and outlook

Significant progress has been attained in the research and development of self-passivating tungsten-based smart alloys for a future fusion power plant. The bulk W-Cr-Y systems, produced by mechanical alloying and compacted via field-assisted sintering technology, show remarkable performance both under regular plasma and under accident conditions. Developed smart alloy solutions now allow for the testing under conditions comparable with lifetime conditions in DEMO power plant. Plasma performance of smart alloys have been tested under plasma particle fluence expected after up to 20 days of the continuous DEMO operation.

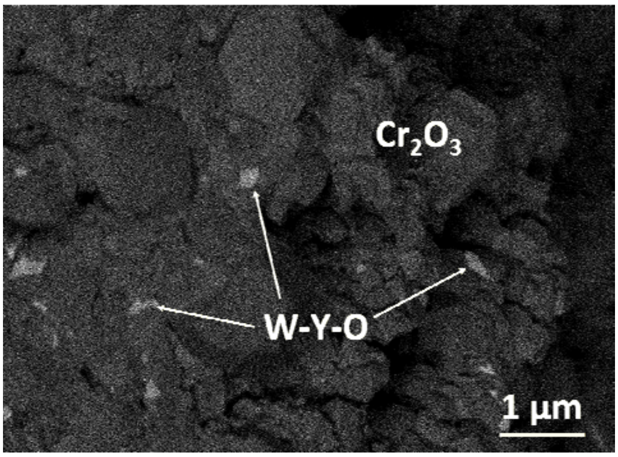

Fig. 3. Surface of W-Cr-Y smart alloy after oxidation in humid atmosphere at 1000°C for 10 days.

Due to the initial selective sputtering of the alloying elements, a layer of pure tungsten has been formed effectively protecting the remaining smart alloy from sputtering by the plasma. As a result, both smart alloys and pure tungsten samples demonstrated to have very similar sputtering resistance given the energies of plasma particles is below the sputtering threshold for W. The detected mass loss of smart alloys and of tungsten was identical to the estimated values, confirming the absence of additional loss of alloying elements in the course of plasma exposure.

Performance of smart alloys was also extensively tested under accident conditions. Studies were made with heated SA samples exposed to the humid air atmosphere as expected in the course of a severe accident in DEMO. Direct measurements of sublimation have been pioneered in the course of this study. Smart alloys demonstrate at least a 40-fold suppression of sublimation as compared to that of pure tungsten. The surface of exposed smart alloy contains less than 1 area % of W-Y mixed oxides. The formation of volatile WO_3 was not detected. The aforementioned experimental findings coupled with a pronounced shape preservation even under accident conditions [9] outline the remarkable progress in R&D on smart alloys.

Certainly, there are still open questions both in physics understanding and in technological development of the smart alloy systems. The role of yttrium in the stabilizing of the W-Cr solid solution is yet to be understood in sufficient details. Our preliminary ab-initio based thermodynamic modelling of phase diagram in ternary W-Cr-Y system showed that in presence of Y, the predicted solute solution temperature in W-Cr sub-system is reduced in a comparison with those found in the corresponding binary alloy. The adverse effects caused by high energy particle sputtering and by seeded plasmas need further investigations. Among the crucial challenges are the thermo-mechanical properties of developed systems. Very important are also technological aspects, such as joining technology for casting smart alloys onto corresponding structural materials and scaling up the manufacturing technology to the industrial level. Last but not least, a complete evaluation of neutron effects, such as transmutation and the assessment of impurity effects on the smart alloy performance, are of highest importance. A dedicated research program has been started at the Forschungszentrum Jülich and the first results are reported in [29].

Acknowledgments

A part of these studies has been carried out within the framework of the EUROfusion Consortium and has received funding from the Euratom research and training programme 2014-2018 and 2019-2020 under grant agreement No. 633053. The views and opinions expressed herein do not necessarily reflect those of the European Commission. The research benefitted from a grant of the European Commission through the Erasmus Mundus International Doctoral College in Fusion Science and Engineering (FUSION-DC). The work at WUT has been carried out as a part of an international project co-financed from the funds of the program of the Polish Minister of Science and Higher Education entitled "PMW" in 2019; Agreement No. 5018/H2020-Euratom/2019/2.

References

[1] N. Taylor, P. Cortes, Lessons learnt from ITER safety & licensing for DEMO and future nuclear fusion facilities, Fusion Eng. Des. 89 (2014) 1995–2000. https://doi.org/10.1016/j.fusengdes.2013.12.030.

[2] N. Taylor, S. Ciattaglia, H. Boyer, D. Coombs, X.Z. Jin, K. Liger, J.C. Mora, G. Mazzini, T. Pinna, E. Urbonavičius, Resolving safety issues for a demonstration fusion power plant, Fusion Eng. Des. 124 (2017) 1177–1180. https://doi.org/10.1016/j.fusengdes.2017.02.018.

[3] M. D, Final Report of the European Fusion Power Plant Conceptual Study (PPCS), EFDA(05)-27/4.10, Garching, 2005.

[4] T. Wegener, F. Klein, A. Litnovsky, M. Rasinski, J. Brinkmann, F. Koch, C. Linsmeier, Development of yttrium-containing self-passivating tungsten alloys for future fusion power plants, Nucl. Mater. Energy. 9 (2016). https://doi.org/10.1016/j.nme.2016.07.011.

[5] F. Koch, H. Bolt, Self passivating W-based alloys as plasma facing material for nuclear fusion, Phys. Scr. T. T128 (2007) 100–105. https://doi.org/10.1088/0031-8949/2007/T128/020.

[6] F. Koch, S. Köppl, H. Bolt, Self passivating W-based alloys as plasma-facing material, J. Nucl. Mater. 386–388 (2009) 572–574. https://doi.org/10.1016/j.jnucmat.2008.12.179.

[7] F. Koch, J. Brinkmann, S. Lindig, T.P. Mishra, C. Linsmeier, Oxidation behaviour of silicon-free tungsten alloys for use as the first wall material, Phys. Scr. T. T145 (2011) 014019. https://doi.org/10.1088/0031-8949/2011/T145/014019.

[8] A. Calvo, C. Garcia-Rosales, N. Ordas, I. Iturriza, K. Schlueter, F. Koch, G. Pintsuk, E. Tejado, J.Y. Pastor, Self-passivating W-Cr-Y alloys : Characterization and testing, 124 (2017) 1118–1121.

[9] A. Litnovsky, T. Wegener, F. Klein, C. Linsmeier, M. Rasinski, A. Kreter, X. Tan, J. Schmitz, J.W. Coenen, Y. Mao, J. Gonzalez-Julian, M. Bram, New oxidation-resistant tungsten alloys for use in the nuclear fusion reactors, in: Phys. Scr., 2017. https://doi.org/10.1088/1402-4896/aa81f5.

[10] J.S. Benjamin, Dispersion strengthened superalloys by mechanical alloying, Metall. Trans. 1 (1970) 2943–2951. https://doi.org/10.1007/BF03037835.

[11] P. López-Ruiz, N. Ordás, S. Lindig, F. Koch, I. Iturriza, C. García-Rosales, Self-passivating bulk tungsten-based alloys manufactured by powder metallurgy, Phys. Scr. T. T145 (2011) 014018. https://doi.org/10.1088/0031-8949/2011/T145/014018.

[12] O. Guillon, J. Gonzalez-Julian, B. Dargatz, T. Kessel, G. Schierning, J. Räthel, M. Herrmann, Field-assisted sintering technology/spark plasma sintering: Mechanisms, materials, and technology developments, Adv. Eng. Mater. 16 (2014) 830–849.

https://doi.org/10.1002/adem.201300409.

[13] F. Klein, T. Wegener, A. Litnovsky, M. Rasinski, X.Y. Tan, J. Gonzalez-Julian, J. Schmitz, M. Bram, J.W. Coenen, C. Linsmeier, Oxidation resistance of bulk plasma-facing tungsten alloys, Nucl. Mater. Energy. 15 (2018). https://doi.org/10.1016/j.nme.2018.05.003.

[14] F. Klein, T. Wegener, A. Litnovsky, M. Rasinski, X. Tan, J. Schmitz, C. Linsmeier, J.W. Coenen, H. Du, J. Mayer, U. Breuer, On oxidation resistance mechanisms at 1273 K of tungsten-based alloys containing chromium and yttria, Metals (Basel). 8 (2018). https://doi.org/10.3390/met8070488.

[15] F. Klein, A. Litnovsky, T. Wegener, X. Tan, J. Gonzalez-Julian, M. Rasinski, J. Schmitz, C. Linsmeier, M. Bram, J.W. Coenen, Sublimation of advanced tungsten alloys under DEMO relevant accidental conditions, Fusion Eng. Des. (2019). https://doi.org/10.1016/j.fusengdes.2019.02.039.

[16] J. Schmitz, A. Litnovsky, F. Klein, T. Wegener, X.Y. Tan, M. Rasinski, A. Mutzke, P. Hansen, A. Kreter, A. Pospieszczyk, S. Möller, J.W. Coenen, C. Linsmeier, U. Breuer, J. Gonzalez-Julian, M. Bram, WCrY smart alloys as advanced plasma-facing materials – Exposure to steady-state pure deuterium plasmas in PSI-2, Nucl. Mater. Energy. 15 (2018). https://doi.org/10.1016/j.nme.2018.05.002.

[17] J. Schmitz, A.M. Litnovsky, F. Klein, X. Tan, U. Breuer, M. Rasinski, S. Ertmer, A. Kreter, J. Gonzalez-Julian, M. Bram, J.W. Coenen, C. Linsmeier, Argon-seeded plasma exposure and oxidation performance of tungsten-chromium-yttrium smart alloys, Tungsten. 1 (2019) 159–168. https://doi.org/10.1007/s42864-019-00016-7.

[18] J. Schmitz, A. Litnovsky, F. Klein, K. De Lannoye, A. Kreter, M. Rasinski, U. Breuer, J. Gonzalez-Julian, M. Bram, J.W. Coenen, C. Linsmeier, On the plasma suitability of WCrY smart alloys-the effect of mixed D+Ar/He plasmas, Phys. Scr. 2020 (2020) 14002. https://doi.org/10.1088/1402-4896/ab367c.

[19] A. Litnovsky, F. Klein, J. Schmitz, T. Wegener, C. Linsmeier, M.R. Gilbert, M. Rasinski, A. Kreter, X. Tan, Y. Mao, J.W. Coenen, M. Bram, J. Gonzalez-Julian, Smart first wall materials for intrinsic safety of a fusion power plant, Fusion Eng. Des. 136 (2018). https://doi.org/10.1016/j.fusengdes.2018.04.028.

[20] A. Kreter, C. Brandt, A. Huber, S. Kraus, S.M.O. Ller, M. Reinhart, B. Schweer, G. Sergienko, B. Unterberg, Linear plasma device PSI-2 for plasma-material interaction studies, Fusion Sci. Technol. 68 (2015) 8–14. https://doi.org/10.13182/FST14-906.

[21] H.J.N. van Eck, G.R.A. Akkermans, S.A. van der Westen, D.U.B. Aussems, M. van Berkel, S. Brons, I.G.J. Classen, H.J. [van der Meiden], T.W. Morgan, M.J. [van van de Pol, J. Scholten, J.W.M. Vernimmen, E.G.P. Vos, M.R. de Baar, High-fluence and high-flux performance characteristics of the superconducting Magnum-PSI linear plasma facility, Fusion Eng. Des. 142 (2019) 26–32. https://doi.org/https://doi.org/10.1016/j.fusengdes.2019.04.020.

[22] H.J. van der Meiden, A.R. Lof, M.A. van den Berg, S. Brons, A.J.H. Donné, H.J.N. van Eck, P.M.J. Koelman, W.R. Koppers, O.G. Kruijt, N.N. Naumenko, T. Oyevaar, P.R. Prins, J. Rapp, J. Scholten, D.C. Schram, P.H.M. Smeets, G. van der Star, S.N. Tugarinov, P.A. van Emmichoven, Advanced Thomson scattering system for high-flux linear plasma generator, Rev. Sci. Instrum. 83 (2012) 123505. https://doi.org/10.1063/1.4768527.

[23] Y. Igitkhanov, B. Bazylev, I. Landman, R. Fetzer, Design Strategy for the PFC in DEMO Reactor, KIT Scientific Report 7637, Karlsruhe, 2013.

[24] J. Schmitz, Development of tungsten alloy plasma-facing materials for the fusion power plant, Ghent University and University of Bochum, 2020.

[25] A. Litnovsky, T. Wegener, F. Klein, C. Linsmeier, M. Rasinski, A. Kreter, X. Tan, J. Schmitz, Y. Mao, J.W. Coenen, M. Bram, J. Gonzalez-Julian, Advanced smart tungsten alloys for a future fusion power plant, Plasma Phys. Control. Fusion. 59 (2017). https://doi.org/10.1088/1361-6587/aa6948.

[26] A. Litnovsky, T. Wegener, F. Klein, C. Linsmeier, M. Rasinski, A. Kreter, B. Unterberg, J.W. Coenen, H. Du, J. Mayer, C. Garcia-Rosales, A. Calvo, N. Ordas, Smart tungsten alloys as a material for the first wall of a future fusion power plant, Nucl. Fusion. 57 (2017). https://doi.org/10.1088/1741-4326/aa6816.

[27] T. Wegener, F. Klein, A. Litnovsky, M. Rasinski, J. Brinkmann, F. Koch, C. Linsmeier, Development and analyses of self-passivating tungsten alloys for DEMO accidental conditions, Fusion Eng. Des. 124 (2017). https://doi.org/10.1016/j.fusengdes.2017.03.072.

[28] ThermoLab website, https://tec.ipp.kfa-juelich.de/thermolab, (access details: Thermolab@fz-juelich.de)

[29] F. Klein, M.R. Gilbert, A. Litnovsky, J. Gonzalez-Julian, S. Weckauf, T. Wegener, J. Schmitz, C. Linsmeier, M. Bram, J.W. Coenen, Tungsten–chromium–yttrium alloys as first wall armor material: Yttrium concentration, oxygen content and transmutation elements, Fusion Eng. Des. 158 (2020) 111667. https://doi.org/10.1016/j.fusengdes.2020.111667.